Anomalous depolarization of the $5p\,^2P_{3/2} \rightarrow 8p\,^2P_{j'}$ transitions in atomic ^{87}Rb

S. B. Bayram, M. D. Havey, D. V. Kupriyanov, and I. M. Sokolov
Department of Physics, Old Dominion University, Norfolk, Virginia 23529
(Received 17 August 1999; published 7 June 2000)

Measurements of the linear polarization degree of the $5p\,^2P_{3/2} \rightarrow 8p\,^2P_{j'}$ transitions ($j'=1/2,3/2$) in atomic ^{87}Rb are reported. The radiative transitions are electric-dipole forbidden, but electric-quadrupole allowed. In addition, because of the relatively strong spin-orbit interaction in Rb, the p-p transitions can acquire a magnetic-dipole transition strength that may be a measurable fraction of the electric-quadrupole strength. The polarization measurements can generally provide a different and sensitive way to extract the relative transition strengths. We have measured the linear polarization degree of the $5p\,^2P_{3/2} \rightarrow 8p\,^2P_{j'}$ transitions over a wide range of Rb density. We report here observations of a different depolarization effect, whereby the measured polarization of the $5s\,^2S_{1/2} \rightarrow 5p\,^2P_{3/2} \rightarrow 8p\,^2P_{1/2}$ transition *increases*, while that for the $5s\,^2S_{1/2} \rightarrow 5p\,^2P_{3/2} \rightarrow 8p\,^2P_{3/2}$ transition *decreases* with increasing Rb density. The behavior is attributed to strong laser field effects associated with the $5s\,^2S_{1/2} \rightarrow 5p\,^2P_{3/2}$ resonance transition.

PACS number(s): 32.70.Cs, 32.70.Fw

INTRODUCTION

The determination of dipole transition matrix elements associated with atomic resonance lines, and with transitions among other low-lying atomic levels, has reached quite a high level of precision. These quantities, which determine radiative lifetimes and branching ratios, observables in atomic parity violation measurements, and dipole electrical polarizability have recently been determined to a precision of a few tenths of a percent in some cases [1–5]. Precision sum rules related to the vector and scalar transition probabilities for excited-state transitions have also been directly measured [6,7]. Alternative experimental approaches to the measurement of the strength of transitions between *excited* levels in atoms have also been proposed or demonstrated [8]. Until quite recently, it has been difficult to measure such quantities to a precision better than typically 10%. In alkali-metal spectra, *forbidden* electronic transitions associated with s-d and p-p transitions have also been observed [9]. However, the determination of such forbidden transition strengths in atomic systems is still a challenging enterprise, and new approaches, as well as refinement of existing ones, are required to make progress in this area [10].

For atomic systems, levels which radiatively decay solely by a forbidden process typically have lifetimes greater than a microsecond or so, but decay times of milliseconds to a second are not uncommon. In one-electron atoms, forbidden transitions are normally those that have multipole character [11] other than electric dipole. Generally, the strength of these weak processes is difficult to accurately compute, and so precise measurement of them provides challenging benchmarks to sophisticated atomic structure calculations. In addition to this, forbidden transitions out of metastable levels can have exceptionally narrow natural widths, and the transitions may serve thus as optical frequency standards or as atomic line filters. These metastable levels can also collect significant populations in strongly pumped atomic or molecular gases, weakly ionized plasmas, or in other collision-dominated gaseous media. Because of collisional quenching, energy pooling, or superelastic collisions with the metastable atoms, such species then play an important role in energy balance for complex systems.

In addition to these general considerations, recent theoretical reports predicted an optical diode behavior associated with an electric dipole-electric quadrupole two-photon excitation in atomic Cs [12]. The intriguing result obtained in those papers was that the two-photon excitation and polarization spectrum associated with the $6s\,^2S_{1/2} \rightarrow 5d\,^2D_j \rightarrow 11p\,^2P_{3/2}$ transition in Cs depends strongly on the relative *propagation* direction of the two beams responsible for the excitation. This optical diode effect is in addition to the corresponding variations in the polarization directions of the two light sources. The effect occurs because of the relative $E2$-$E1$ sign change upon reversal of the wave vector **k**.

In the present paper, we report on an experimental study of the two-photon $5s\,^2S_{1/2} \rightarrow 5p\ \ ^2P_{3/2} \rightarrow 8p\,^2P_{j'}$ transitions in atomic Rb. In this case, the p-p transition is electric dipole ($E1$) forbidden, but has allowed magnetic-dipole ($M1$) and electro-quadrupole ($E2$) amplitudes. The $M1$ amplitude is generated by off-diagonal (in n) spin-orbit mixing of the np multiplets, an effect characteristic of the heavier alkali-metal atoms. Other effects associated with departures from hydrogenic behavior, including inversion of the ordering of the fine-structure multiplet ordering with j [13], and strong perturbation of the relative electric-dipole multiplet transition strengths in the $5s\,^2S_{1/2} \rightarrow n'p\,^2P_{j'}$ principal series in K, Rb, and Cs have also been observed [14–16]. In the present study, we show and then exploit the fact that the $E2$ and $M1$ contributions to the transition probability are distinguished by different linear polarization dependence of the excitation rates. This circumstance can generally allow the relative size of the $M1$ and $E2$ transition strengths to be determined. However, in the current paper, we focus on transitions to the $8p\,^2P_{j'}$ levels, with $j'=1/2$ and 3/2, with particular attention paid to an unusual Rb density dependence of the measured linear polarization degree.

In the following paragraphs, we first lay out in detail the general approach and basic experimental scheme. This is followed by the experimental results and a discussion of various

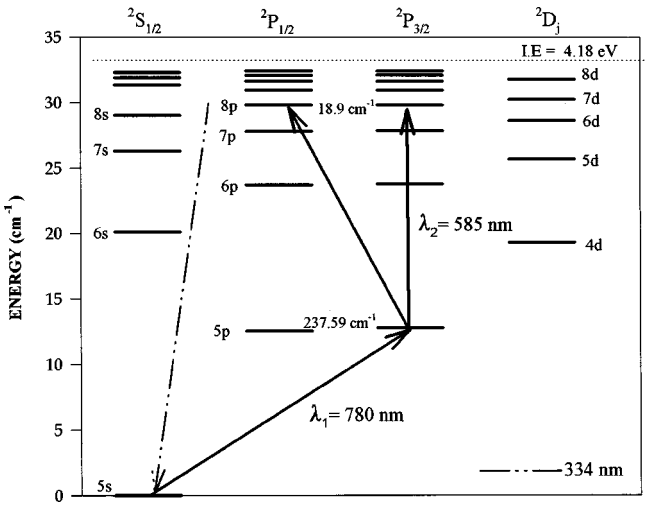

FIG. 1. Energy-level diagram of atomic Rb, showing the transitions used in the experiment. I.E. is the ionization energy.

systematic effects, the most important of which is a strong variation of the measured depolarization with Rb density.

EXPERIMENTAL DETAILS

The general scheme of the experiment is shown in Fig. 1. There the $5s\,^2S_{1/2}\rightarrow 5p\,^2P_{3/2}$ transition is resonantly excited by linear polarized light from laser 1. Stepwise excitation by laser 2 on the $5p\,^2P_{3/2}\rightarrow 8p\,^2P_{j'}$ transitions promotes atoms to the $8p\,^2P_{j'}$ levels. As the laser-2 frequency is varied, the size of the fluorescence signal on the $8p\,^2P_{j'}\rightarrow 5s\,^2S_{1/2}$ transitions serves as a signature of the resonance condition. The rate of promotion of atoms to the $8p\,^2P_{j'}$ levels depends also on the polarization of laser 2. In the present experiment, laser 2 is linearly polarized and is directed along or perpendicular to the polarization direction of laser 1. The geometry and coordinates are illustrated in Fig. 2. When the two polarization directions are collinear, the signal is defined as $I_{\parallel}$. If they are perpendicular, the signal is $I_{\perp}$. In terms of these measured intensities, a linear polarization degree for the process may be defined as

$$P_L=\frac{I_{\parallel}-I_{\perp}}{I_{\parallel}+I_{\perp}}. \tag{1}$$

It is important to point out that the measured value of P_L normally depends on systematic factors such as collisions, stray magnetic or electric fields, and hyperfine depolarization in the $5p\,^2P_{3/2}$ level. Such effects are mitigated in the present experiment by using pulsed laser excitation and by adjusting the temporal overlap of the pulses to $\sim$1 ns. A further discussion of each of these factors is made in a later section of this paper.

A schematic diagram of the experimental apparatus is shown in Fig. 3. There, a neodymium-doped yttrium aluminum garnet (Nd:YAG) pump laser operating at 10 Hz is used to pump two dye lasers. The laser-1 oscillator is of the grazing incidence design and operates at the fixed wavelength of the Rb D2 line at 780 nm. It has a bandwidth of approxi-

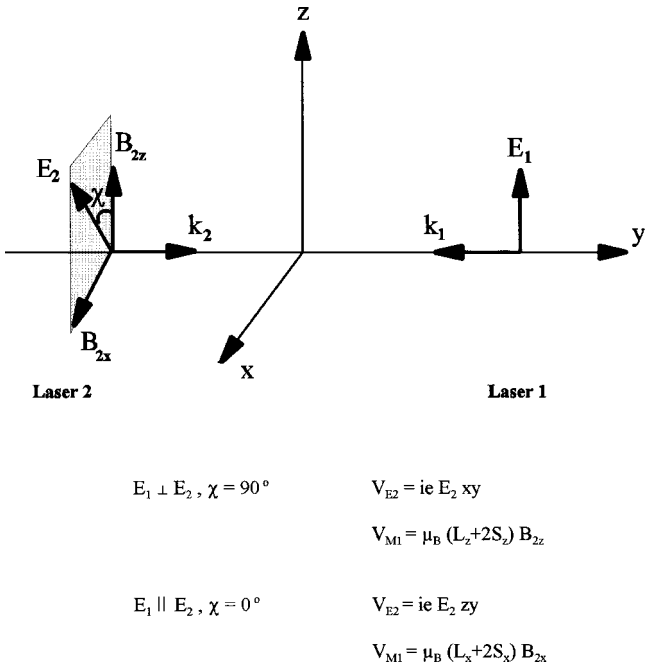

FIG. 2. Geometry of the experimental excitation scheme, defining the polarization and propagation directions of the laser beams used in the experiment.

mately 2 cm^{-1}. Output power from the oscillator is increased by about a factor of 10 in a single stage of amplification, generating approximately 100 μJ in an $\sim$5 ns pulse. The laser-1 output is highly linearly polarized. A second grazing incidence laser oscillator produces light in the vicinity of the $5p\,^2P_{3/2}\rightarrow 8p\,^2P_{j'}$ transitions around 570 nm. With a single stage of amplification, the output power of laser 2 is about 500 μJ in a bandwidth of $\sim$0.5 cm^{-1}. The output frequency of laser 2 may be continuously varied over a range of around 20 cm^{-1} by computer-controlled motorized rotation of the tuning mirror mounting stage. This permits scanning over either of the $5p\,^2P_{3/2}\rightarrow 8p\,^2P_{j'}$ transitions, or over the entire fine-structure multiplet splitting of 18.9 cm^{-1}. A portion of the laser-2 output is passed through an étalon of free-spectral-range 3.3 cm^{-1} and a finesse of about 100. The transmission of the étalon is detected by a photodiode; the signal serves as a monitor of the spectral length of the laser-2 scan. The linearly polarized main output beam from laser 2 has its linear polarization direction adjusted to be collinear with that of laser 1 by a Glan-Thompson prism polarizer, which is mounted in a precision mechanical rotation stage. A liquid-crystal variable retarder (LCR) is then used to electronically vary the linear polarization direction to be collinear or perpendicular to that of laser 1. The polarimeter has a typical analyzing power $A>0.999$. It should be noted that the retardance of the LCR can in principle depend on laser intensity, in part because of transient thermal effects on the retardance. However, in the present experiment, measurement of the analyzing power was made at the largest laser intensity used in the experiments; under these conditions, no such effects were observed.

The two laser beams pass collinearly, but in opposite directions, through a nonmagnetic heated oven that houses a

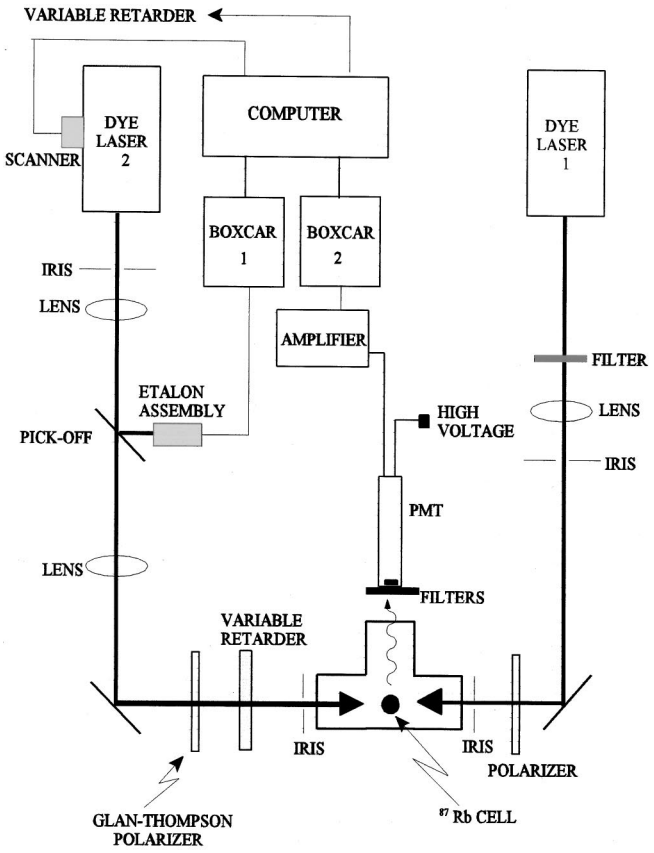

FIG. 3. Schematic diagram of the experimental apparatus.

Pyrex sample cell containing ^{87}Rb vapor. The oven temperature is controlled to about 0.1 K and is varied in the range 325–425 K, corresponding to a Rb vapor density in the range $\sim 10^{11}-10^{13}\,\mathrm{cm}^{-3}$. Fluorescence signals are detected at right angles to the laser beams by a photomultiplier tube (PMT) mounted with interference and colored-glass filters that pass the $8p\,^2P_{j'} \rightarrow 5s\,^2S_{1/2}$ signal radiation, which has a wavelength of 335 nm. The filters reject with very high efficiency the Nd:YAG laser light and the intense radiation from laser 1 and laser 2. The PMT output is amplified and processed in a boxcar averager operating in a sample-and-hold mode, where the average single-shot output level within the detection gate is digitized and stored in a laboratory computer for later analysis. Control of the laser-2 scan, the polarization direction of laser 2, the registration of the étalon transmission signal, and the boxcar signal levels are all managed by a computer-controlled data acquisition system. A typical scan over the $8p$ fine-structure multiplet when the cell temperature is 326 K is shown in Fig. 4.

GENERAL ANALYSIS

The main results of the experiment are expressed in terms of a *linear polarization degree* for the $5s\,^2S_{1/2} \rightarrow 5p\,^2P_{3/2} \rightarrow 8p\,^2P_{j'}$ transitions. We focus in this study on transitions through the $5p\,^2P_{3/2}$ level only, for it may be readily aligned by optical excitation, while the $5p\,^2P_{1/2}$ level can support no alignment. For radiative transitions through the $5p\,^2P_{3/2}$

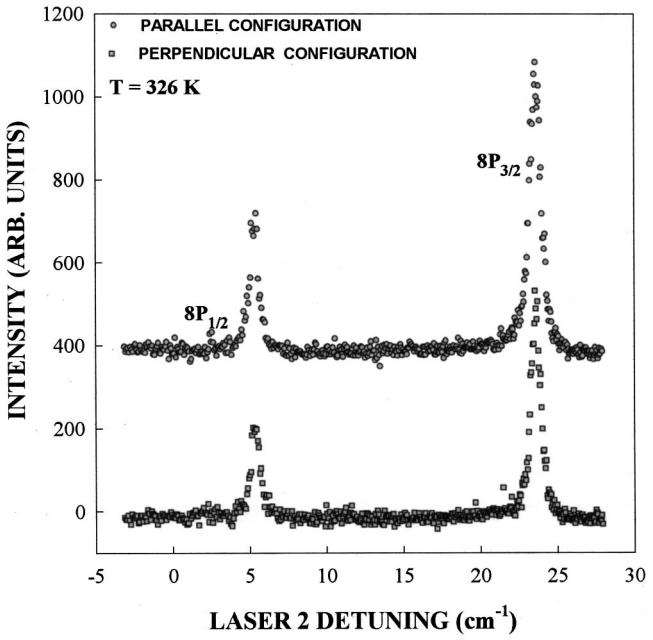

FIG. 4. Scan over the $5p\,^2P_{3/2} \rightarrow 8p\,^2P_j$ transitions in ^{87}Rb, showing the polarization dependence of the transition rate. The parallel configuration data have been offset by 400 units. These data were taken at $T = 326$ K.

level, which is aligned by linearly polarized excitation with laser 1, the linear polarization degree provides a sensitive measure of the mixture of the different multipoles contributing to the transition. The relevant expressions describing these contributions are presented in the following paragraphs. We point out that it is also possible to orient each multiplet component with a circularly polarized laser 1, and then determine a circular polarization degree for the $5p\,^2P_j \rightarrow 8p\,^2P_{j'}$ transitions. This approach will be discussed in a later paper.

The transition operator for the p-p transition may be written as [17]

$$V = -\boldsymbol{\mu}\cdot\mathbf{B} - ie\mathbf{E}\cdot\mathbf{rk}\cdot\mathbf{r}. \tag{2}$$

In the expression, $\mathbf{E}$ and $\mathbf{B}$ are the amplitudes of the field driving the transition, which in the present case is laser 2. The operator $\mathbf{r}$ represents the electron position, and $\boldsymbol{\mu} = \mu_b(\mathbf{L} + g_s\mathbf{S})$, where $\mathbf{L}$ and $\mathbf{S}$ are the electron orbital and spin angular momentum, $g_s = 2.002\,32$ is the electron g factor, and μ_b is the Bohr magneton. The magnitude of the field amplitudes are related by $E = B/c$, where c is the speed of light in a vacuum. It is convenient to represent the operators in Eq. (1) in irreducible tensor form [18]. The components of these operators, relevant to the geometry of the present experiment, as shown in Fig. 2, are presented in Table I, along with the associated selection rules on the total angular-momentum quantum numbers j and m_j.

The expressions in Table I may be used to obtain the linear polarization degree for the $5s\,^2S_{1/2} \rightarrow 5p\,^2P_{3/2} \rightarrow 8p\,^2P_{j'}$ transitions for purely magnetic-dipole and electric-quadrupole transitions. The values are summarized in Table II. The limiting polarization values, which define a

TABLE I. Irreducible tensor operators, relevant multipole transition, and selection rules on the total angular momentum J^2 and component J_z for the parallel and perpendicular geometries of the present study.

Cartesian operator	Irreducible equivalent	M-selection rules	J-selection rules
$\mu_z\,(M1)$	μ_0^1	$\Delta m=0$	$\Delta j=0,\pm1$
$\mu_x\,(M1)$	$1/\sqrt{2}(\mu_{-1}^1-\mu_1^1)$	$\Delta m=\pm1$	$\Delta j=0,\pm1$
$z\,(E1)$	r_0^1	$\Delta m=0$	$\Delta j=0,\pm1$
$zy\,(E2)$	$i/2(r_{-1}^2+r_1^2)$	$\Delta m=\pm1$	$\Delta j=0,\pm1,\pm2$
$xy\,(E2)$	$i/2(r_{-2}^2-r_2^2)$	$\Delta m=\pm2$	$\Delta j=0,\pm1,\pm2$

useful baseline for discussion of the experimental results, assume that the alignment of the $5p\,^2P_{3/2}$ level is not disturbed by the effects of collisions, radiation trapping, or hyperfine precession [19] or external fields. The influence of these, and other effects, is discussed in the following section.

More generally, the linear polarization is conveniently expressed in terms of the axially symmetric electronic alignment component [20]. This component, produced in the present experiment by excitation of the $5s\,^2S_{1/2}\rightarrow5p\,^2P_{3/2}$ transition with linearly polarized light, is defined as

$$\langle A_0\rangle=\frac{\langle 3J_z^2-J^2\rangle}{J(J+1)}, \tag{3}$$

where $\langle\,\rangle$ indicates an average value over the magnetic sublevels of the $5p\,^2P_{3/2}$ level. For linearly polarized excitation of the $5p\,^2P_{3/2}$ level, the alignment is $-\frac{4}{5}$.

As indicated in the Introduction, the spin-orbit interaction in the heavier alkali-metal atoms produces mixing of the $np\,^2P_j$ levels with the same j. As discussed originally by Fermi [21], and more recently by others [22], this effect is partly responsible for the strong departure of the spin-orbit doublet intensity ratios from the value of 2 expected in the absence of spin-orbit interaction. We point out a second effect, one that is of interest in the present work; the spin-orbit interaction generates a nonzero magnetic-dipole amplitude for radiative transitions between different $np\,^2P_j$ levels. This amplitude is in addition to the normally expected electric-quadrupole contribution. The relative strength of the electric-quadrupole to magnetic-dipole intensity may be parametrized by a ratio $R_{j'}$ which is defined as the ratio of total intensities for the $E2$ and $M1$ transitions. In terms of the alignment $\langle A_0\rangle$ and R_j, the mixed multipole linear polarization degree may be parametrized for the $5p\,^2P_{3/2}\rightarrow8p\,^2P_{1/2}$ transition as

$$P_L=\frac{15\langle A_0\rangle(1-R)}{16(1+R)-5\langle A_0\rangle(1-R)}, \tag{4}$$

and for the $5p\,^2P_{3/2}\rightarrow8p\,^2P_{3/2}$ transition as

$$P_L'=\frac{-15\langle A_0\rangle}{20+5\langle A_0\rangle+20R'} \tag{5}$$

Note that the mixed multipole ratio R (R') will generally be different for the two transitions. In addition, the alignment in the $5p\,^2P_{3/2}$ level can depend on Rb density and laser power, and can also be modified by hyperfine depolarization and collisions in the $5p$ levels. However, it is interesting to note that a polarization ''invariant'' may be obtained by eliminating $\langle A_0\rangle$ from the two equations:

$$\left(\frac{P_L}{P_L+3}\right)\left(\frac{P_L'+3}{P_L'}\right)=\frac{5}{4}\frac{(R-1)}{(R+1)}(R'+1). \tag{6}$$

The quantities R and R' are ratios of the total intensities for the $E2$ and $M1$ transitions. They may be obtained from the general intensity expressions for $M1$ and $E2$ transitions given by several authors [11], and are given in atomic units by

$$I(M1)=\frac{1}{3}\frac{k^3}{c^2}\frac{|M|^2}{2J_i+1}, \tag{7}$$

$$I(E_2)=\frac{1}{15}k^5\frac{|Q|^2}{2J_i+1}. \tag{8}$$

In the above expressions, k is the wave vector, c the speed of light, and M and Q are reduced transition matrix elements for the magnetic dipole and electric quadrupole transitions. J_i is the angular momentum of the initial level.

TABLE II. Maximum linear polarization degrees in percent for pure multipole transitions. The initial level has angular momentum j, while for $M1$ and $E2$ transitions the final angular momentum is j'. For $E1$ transitions, the final level is indicated in the column. X indicates that the transition is not permitted.

j	j'	$M1$	$E2$	$E1(^2S_{1/2})$
1/2	1/2	0	X	0
1/2	3/2	0	0	0
3/2	1/2	−60	+100	+60
3/2	3/2	+75	0	+60

RESULTS AND DISCUSSION

The measured linear polarization values were found to be independent of the power of either laser (at high density), stray electric or magnetic fields, and variation in the intensity of the fluorescence signal. At a lower density, the measured polarization was measurably free of variation due to changes in laser-2 power, but varied weakly, for low powers, with laser-1 power. However, as shown in Figs. 5 and 6, there was a strong dependence on the cell temperature, which we attribute to the changing Rb density with temperature. In particular, the most striking feature of the data is that the linear polarization degree for the $5s\,^2S_{1/2}\rightarrow5p\,^2P_{3/2}\rightarrow8p\,^2P_{1/2}$ transition *increases* with increasing Rb density, while that for the $5s\,^2S_{1/2}\rightarrow5p\,^2P_{3/2}\rightarrow8p\,^2P_{3/2}$ transition *decreases*. In each case, the measured linear polarization goes to a sensibly constant value at higher Rb density. The variation are quite unusual, particularly for the $5s\,^2S_{1/2}\rightarrow5p\,^2P_{3/2}\rightarrow8P\,^2P_{1/2}$

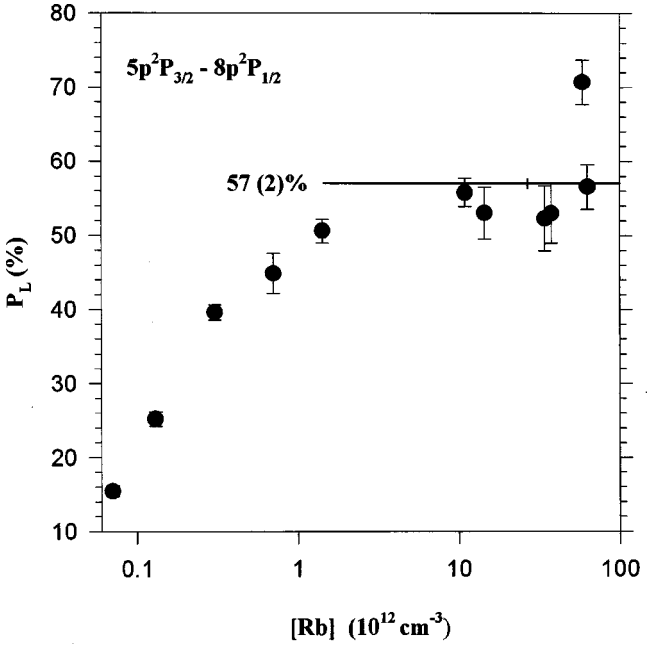

FIG. 5. Rubidium density dependence of the measured linear polarization degree for the $5s\ ^2S_{1/2}\rightarrow 5p\ ^2P_{3/2}\rightarrow 8p\ ^2P_{1/2}$ transition.

transition, for most systematic effects associated with density, such as an increased collision rate or radiation trapping, lead to decrease in polarization. Within the measurement uncertainty, this behavior demonstrated no strong dependence on the intensity of laser 2, and showed no observable dependence on applied static electric or magnetic-field strength. In addition, the density dependence is inconsistent with the polarization invariant of Eq. (6), demonstrating that the dependence is not simply due to variation in the $5p\ ^2P_{3/2}$ level alignment with density.

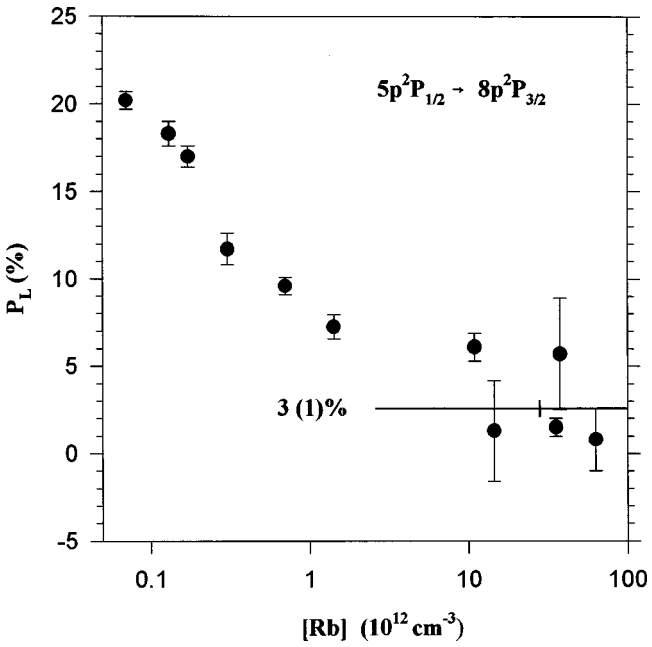

FIG. 6. Rubidium density dependence of the measured linear polarization degree for the $5s\ ^2S_{1/2}\rightarrow 5p\ ^2P_{3/2}\rightarrow 8p\ ^2P_{3/2}$ transition.

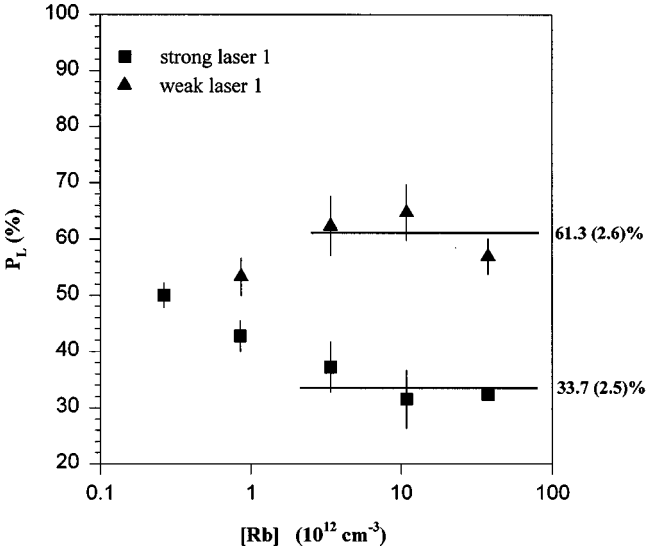

FIG. 7. Rubidium density dependence of the measured linear polarization degree for the $5s\ ^2S_{1/2}\rightarrow 5p\ ^2P_{3/2}\rightarrow 9s\ ^2S_{1/2}$ transition, and for low and high laser-1 power.

The approach of the polarization to nearly constant values at higher Rb density may be explained as follows. At higher densities, the vapor is optically thick to the laser-1 pump radiation, and only the near wings of the laser-1 spectral profile penetrate the vapor to the interaction region of the cell. Thus the two-step process $5s\ ^2S_{1/2}\rightarrow 5p\ ^2P_{3/2}\rightarrow 8p\ ^2P_j$ occurs via the *nonresonant* population of the final state. If the vapor is optically thick enough, then there is minimal population produced in the intermediate level, so collisions, hyperfine pumping, hyperfine quantum beats, and radiation trapping have a negligible effect on the polarization. Evidence supporting this interpretation was found by measuring the linear polarization degree of the $5s\ ^2S_{1/2}\rightarrow 5p\ ^2P_{3/2}\rightarrow 9s\ ^2S_{1/2}$ electric-dipole-allowed transition, for which the linear polarization is known to be 60% in the absence of depolarizing effects in the intermediate level [6]. As shown in Fig. 7, the polarization for weak laser 1 is consistent with the expected value. For higher power, it is interesting that the linear polarization decreases. This effect likely results from laser 1 burning through the vapor at high laser power, thus generating resonantly excited atoms in the interaction region. These atoms are probed by laser 2, resulting in a decrease in polarization due to collisions, radiating trapping, and hyperfine quantum beats. At low density the effect disappears, consistent with the interpretation. Direct measurement of transmitted power of laser 1 showed an approximately 30% decrease as the temperature increased over the range of the measurements, also supporting the idea that excitation was predominately nonresonant. Finally, the data of Figs. 5 and 6 were taken with relatively low laser power, maintained at the level consistent with the proper limiting polarization value of 60% determined in the $5s\ ^2S_{1/2}\rightarrow 5p\ ^2P_{3/2}\rightarrow 9s\ ^2S_{1/2}$ transition measurements.

A possible explanation for the density-dependent variations is that they are caused by secondary effects: reduction in the laser-1 power and modification of its spectral profile in the interaction region due to increased absorption with tem-

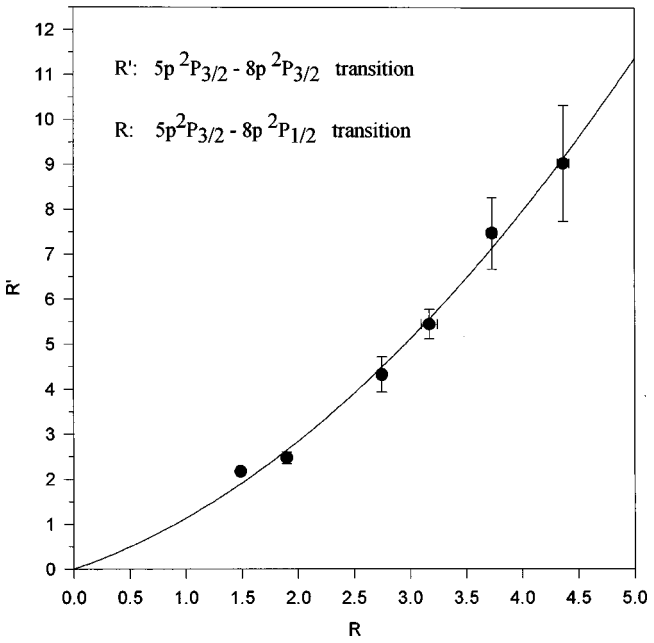

FIG. 8. Relationship between measured total intensity ratios R and R' for the $5s\,^2S_{1/2}\rightarrow 5p\,^2P_{3/2}\rightarrow 8p\,^2P_{1/2}$ and $5s\,^2S_{1/2}\rightarrow 5p\,^2P_{3/2}\rightarrow 8p\,^2P_{3/2}$ transitions, respectively. The curve represents a quadratic fit to the data, as discussed in the text.

perature. The observations discussed in the previous paragraphs suggest this. In addition, as the $M1$ transition probability for the transition is weak, it is sensitive to what would normally by small perturbations generated by high laser power. In this case, qualitative examination of the data indicates that the behavior of the polarization can be due to an increase in the $M1$ transition strength as the density decreases and the laser-1 power in the interaction region increases. We have modeled the ratios of total intensity R and R' by allowing the $M1$ strength to be dependent on laser-1 power. In the model, a natural $M1$ strength is also included for the $5s\,^2S_{1/2}\rightarrow 5p\,^2P_{3/2}\rightarrow 8p\,^2P_{1/2}$ transition, but not for the $5s\,^2S_{1/2}\rightarrow 5p\,^2P_{3/2}\rightarrow 8p\,^2P_{3/2}$ transition, consistent with the expectations of perturbation theory; when $\Delta j=0$ for spin-orbit-induced transitions, the transition amplitude is zero. The model may be compared with the data by eliminating the laser power dependence between R and R', and fitting the result to the R and R' experimental data as extracted from the polarization measurements. The result of this procedure is illustrated in Fig. 8, where very good agreement is found between the fit and the data. Of course, the empirical model used here is only suggestive of one possible explanation for the observations, and further theoretical investigation is clearly needed.

The nearly constant value for the measured polarization at high Rb density suggests that we can obtain values for R and R' from the data. These numbers are presented in Table III, and the values of $R=4.3(3)$ and $R'=24(8)$ are consistent with the expectation that the $M1$ strength is much smaller for the $5p\,^2P_{3/2}\rightarrow 8p\,^2P_{3/2}$ transition than for the $5p\,^2P_{3/2}\rightarrow 8p\,^2P_{1/2}$ transition. These results may be compared to theoretical estimates by finding approximate values for the electric-quadrupole and magnetic-dipole matrix elements. Such $E2$ and $M1$ matrix elements for the $5p\,^2P_{3/2}\rightarrow 8p\,^2P_j$ transitions have been calculated by Derevianko [23] using a fully relativistic coupled cluster approach, and combined to form theoretical values for the ratios R and R'. These values are shown in Table III. Also given in the table are quadrupole matrix elements found by a variation of the Bates-Damgaard method [24,25]. As expected, the $E2$ matrix elements are in very good mutual agreement, supporting the argument that the fundamental disagreement is in the strength of the magnetic-dipole transitions. Accurate values for magnetic-dipole transition matrix elements are generally more difficult to obtain, although estimates may be made from perturbation theory [21,22]. The theoretical estimates for R and R', as shown in Table III, are considerably larger than the experimental results, but the relative sizes of the values for the two multiplet transitions are consistent. Although it is clear that further study is required, the $M1$ matrix elements are difficult to calculate and are generally subject to systematic difficulties [26]. In addition, it is clear that the high-density values for R and R' we have used must be qualified, in that they may contain a residual laser power dependence not accounted for in the empirical model used. Nevertheless, further experimental and theoretical study of the p-p multiplet polarization spectra in the alkali-metal atoms should be motivated by the results.

CONCLUSIONS

Calculations of general expressions for the linear polarization degree of mixed multipole magnetic-dipole and electric-quadrupole transitions for np-$n'p'$ one-electron multiplets have been presented. These expressions are parametrized in terms of the relative total intensities of the individual multipole transitions. Particular application of these results has been made to measurements of the linear polarization degree of the $5s\,^2S_{1/2}\rightarrow 5p\,^2P_{3/2}\rightarrow 8p\,^2P_j$ transitions in ^{87}Rb. The measurements suggest that the strength for each transition may contain significant magnetic-dipole

TABLE III. Summary of experimental results and parameters used to obtain them.

Parameter	$5p\,^2P_{3/2}\rightarrow 8p\,^2P_{1/2}$ transition	$5p\,^2P_{3/2}\rightarrow 8p\,^2P_{3/2}$ transition
$R_{j'}$ (experiment)	4.3(3)	24(8)
$R_{j'}$ (theory)	2400	7.9×10^7
Q_{85} (units of a_0^2) (Bates-Damgaard)	-6.4	-6.4
$\lvert Q_{85}\rvert$ (units of a_0^2) (coupled cluster)	7.31	7.30

and electric-quadrupole contributions. For the $5s\,^2S_{1/2} \rightarrow 5p\,^2P_{3/2} \rightarrow 8p\,^2P_{1/2}$ transition, the strength of the magnetic-dipole amplitude obtained is of comparable size to that of the electric quadrupole, and is considerably larger than expected, based on calculations by Derevianko [23]. We have also observed a strong and anomalous density dependence of the measured polarization values on the $5s\,^2S_{1/2} \rightarrow 5p\,^2P_{3/2} \rightarrow 8p\,^2P_{1/2}$ and $5s\,^2S_{1/2} \rightarrow 5p\,^2P_{3/2} \rightarrow 8p\,^2P_j$ transitions. This unusual effect is attributed to the enhancement of the $M1$ transition probability by the strong $5s\,^2S_{1/2} \rightarrow 5p\,^2P_{3/2}$ resonance radiation. At high density the effect disappears, consistent with a model of the process, allowing the estimation of the relative $E2$ and $M1$ transition matrix elements.

ACKNOWLEDGMENTS

We acknowledge the financial support of the National Science Foundation (Grant No. PHY-9732133) and the U.S. Civilian Research and Development Foundation (Grant No. RP1-263).

[1] Dirk Goebel and Uwe Hohm, Phys. Rev. A **52**, 3691 (1995); M. A. Kadar-Kallen and K. D. Bonin, Phys. Rev. Lett. **72**, 828 (1994).
[2] C. R. Ekstrom, J. Schmiedmayer, M. S. Chapman, T. D. Hammond, and D. E. Pritchard, Phys. Rev. A **51**, 3883 (1995); W. I. McAlexander, E. R. I. Abraham, N. W. M. Ritchie, C. J. Williams, H. T. C. Stoof, and R. G. Hulet, *ibid.* **51**, R871 (1995).
[3] C. W. Oates, K. R. Vogel, and J. L. Hall, Phys. Rev. Lett. **76**, 2866 (1996).
[4] R. J. Rafac, C. E. Tanner, A. E. Livingston, K. W. Kulka, J. G. Berry, and C. A. Kurtz, Phys. Rev. A **50**, R1976 (1994); L. Young, W. T. Hill III, S. J. Sibener, S. D. Price, C. E. Tanner, C. E. Wieman, and S. R. Leone, *ibid.* **50**, 2174 (1994).
[5] U. Volz, M. Jajerus, H. Liebel, A. Schmitt, and H. Schmoranzer, Phys. Rev. Lett. **76**, 2862 (1996).
[6] R. P. Meyer, A. I. Beger, and M. D. Havey, Phys. Rev. A **55**, 230 (1997).
[7] A. I. Beger, M. D. Havey, and R. P. Meyer, Phys. Rev. A **55**, 3780 (1997).
[8] M. D. Havey, Phys. Lett. A **240**, 219 (1998).
[9] See, for examples, M. Lambropoulos, S. E. Moody, S. J. Smith, and W. C. Lineberger, Phys. Rev. Lett. **35**, 159 (1975); P. Lambropoulos, G. Doolen, and S. P. Rountree, *ibid.* **34**, 636 (1975); P. Lambropoulos and M. R. Teague, J. Phys. B **9**, 587 (1976).
[10] E. Biemont and C. J. Zeippen, J. Phys. IV **1**, C1 (1973).
[11] A. Corney, *Atomic and Laser Spectroscopy* (Oxford University Press, New York, 1977); I. B. Levinson and A. A. Nikitin, *Handbook for Theoretical Computation of Line Intensities in Atomic Spectra* (Israel Program for Scientific Translations, Jerusalem, 1965).
[12] Boris Dobrydnev and Mark Havey, Phys. Rev. A **52**, 4010 (1995).
[13] E. Luc-Koenig, Phys. Rev. A **13**, 2114 (1976).
[14] A. A. Radzig and B. M. Smirnov, *Reference Data on Atoms, Molecules, and Ions* (Springer-Verlag, Berlin, 1985).
[15] E. Caliebe and K. Niemax, J. Phys. B **12**, L45 (1979).
[16] L. N. Shabanova and A. N. Khlyustalov, Opt. Spectrosc. **56**, 128 (1984).
[17] M. Weissbluth, *Atoms and Molecules* (Academic, New York, 1979).
[18] M. E. Rose, *Elementary Theory of Angular Momentum* (Wiley, New York, 1957).
[19] K. Blum, *Density Matrix Theory and Applications* (Plenum, New York, 1981).
[20] C. H. Greene and R. N. Zare, Annu. Rev. Phys. Chem. **33**, 119 (1982).
[21] E. Fermi, Z. Phys. **59**, 680 (1930).
[22] For example, see Jon C. Weisheit, Phys. Rev. A **5**, 1621 (1972).
[23] A. Derevianko (private communication).
[24] D. V. Kupriyanov and I. M. Sokolov (unpublished).
[25] D. R. Bates and A. Damgaard, Philos. Trans. R. Soc. London **242**, 101 (1949).
[26] W. van Orden (private communication).